Remarkable optical-potential systematics for lighter heavy ions

M. E. Brandan
Instituto de Física, Universidad Nacional Autónoma de México, Apartado Postal 20-364, México 01000 Distrito Federal, Mexico

K. W. McVoy
Physics Department, University of Wisconsin, Madison, Wisconsin 53706
(Received 22 April 1996)

Nuclear rainbows, which appear in the elastic scattering angular distributions for certain combinations of lighter heavy ions like $^{12}C+^{12}C$ and $^{16}O+^{16}O$, uniquely determine the major features of the optical potentials for these systems. These features are conveniently summarized by the central depth of the real part of the potential, $V(r=0)\sim 100-300$ MeV, and by the ratio of imaginary to real parts of the potential, $W(r)/V(r)$, found to be $\ll 1$ for both small and large r (internal and far-tail transparency), but ≈ 1 in the surface region. The resulting maximum in W/V, which is found over the entire energy range 6 MeV $\lesssim E_L/A \lesssim 100$ MeV, appears to correlate with the peripheral reactions that occur in this energy range. At higher energies the data available indicate that the far-surface region is no longer transparent. Rather, $W\approx V$ there, suggesting the dominance of nuclear knockout reactions in the far tail. The knockout mode of inelasticity is the one described by the double-Glauber approximation, and $W(r)\approx V(r)$ agrees with the Glauber prediction in the high-energy range. This suggests that the double-Glauber prediction begins to be accurate in the low-density tail of the A_1+A_2 interaction around $E_L/A\approx 100$ MeV and that its failure for the higher-density interior may provide a means of investigating the density dependence of Pauli blocking on NN scattering in the nuclear medium. By way of contrast, systems like $^{20}Ne+^{12}C$ and $^{14}N+^{12}C$, which do not exhibit rainbows, have distinctly more absorptive potentials and do not follow the above systematics. This suggests that the imaginary part of the optical potential reflects the shell structure of the target and/or projectile in important ways, and so will not be easy to calculate from an infinite-matter many-body approach. [S0556-2813(96)00410-4]

PACS number(s): 25.70.−z, 24.10.Ht, 25.60.−t

I. INTRODUCTION

The nuclear rainbows seen in the elastic-scattering angular distributions for certain combinations of lighter heavy ions unambiguously determine the major features of V_{opt}, the optical potential for these systems [1–6]. The potentials are by no means static, but evolve with bombarding energy and vary with the ion pairs (A_1+A_2) involved, in a manner which reflects both the structure of A_1 and A_2 and the reactions emanating from this entrance channel.

This information is not of long standing. Although primitive guesses at heavy-ion optical potentials were extracted from even the earliest elastic scattering experiments, it soon became apparent that the low energies and limited angular ranges then available admitted such extreme potential ambiguities that these early data determined little more than the values of the real and imaginary parts of V_{opt} over a narrow radial region near the surface of the system [7]. The situation has improved greatly over the past 10 years, almost entirely as a result of good large-angle data and of the appearance of nuclear rainbows in several light-ion systems at many bombarding energies. For these systems the remaining potential ambiguities have been reduced to fine details of their deep interiors. Stimulated by this recent (and growing) availability of reliable potentials and by the obvious need to extrapolate them to nearby exotic nuclei as many radioactive beams become available, our purpose here is to review the current body of established potentials, presenting them in a manner that exhibits their systematic dependence on both (A_1+A_2) and on the bombarding energy.

These potential systematics seem to be most clearly evident in a single function that we might call the ''reduced imaginary potential,''

$$w(r)\equiv W(r)/V(r), \tag{1}$$

i.e., the ratio of the imaginary and real parts of the optical potential. The choice of name for $w(r)$ is motivated by the fact that the radial shape of $V(r)$ directly reflects the matter distributions of A_1 and A_2 (i.e., is very close to the double-folding potential) [8], and so provides a physically meaningful normalization function for $W(r)$. $W(r)$ itself provides the radial weighting of flux removal or absorption from the entrance channel. As the typical examples shown in Fig. 1 illustrate, its shape is distinctly and consistently very different from that of $V(r)$, and $w(r)=W/V$ provides a useful measure of this difference, by exhibiting the ratio of the absorption $W(r)$ to the matter distribution itself. In addition, $w(r)$ provides a contact with the Glauber approximation, since, as the previous article explains, the simplest form of this approximation predicts that $w(r)\approx 1$, independent of r, for energies below ~100 MeV/nucleon.

Section II of this article presents the characteristics of the heavy-ion potentials, and in Sec. III their uniqueness is discussed. Section IV contains the evidence for the $w(r)$ systematics and Sec. V presents their relation to the Glauber approximation. Section VI concludes with an overview of the systematics and with conjectures about their physical significance.

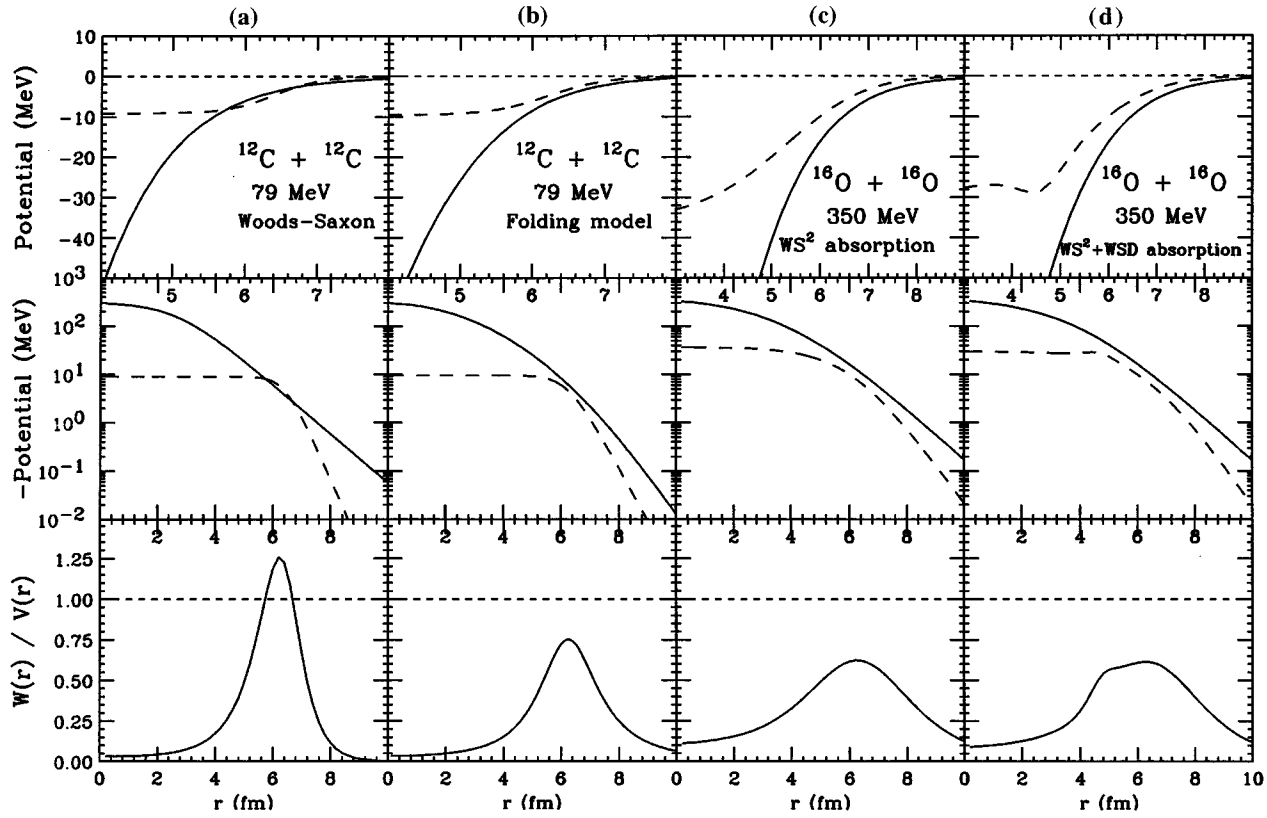

FIG. 1. Typical potentials considered in this study. (a) Woods-Saxon shape for $V(r)$ and $W(r)$ [29]; (b) folding model real part calculated with DDM3Y effective interaction and Woods-Saxon imaginary part [29]; (c) Woods-Saxon squared real and imaginary parts [2]; (d) Woods-Saxon squared real and imaginary parts plus Woods-Saxon derivative absorption [11].

II. POTENTIAL SYSTEMATICS IN BRIEF

As we illustrate in more detail below, the $w(r)$ curves shown in Fig. 1 for $^{12}C+^{12}C$ and $^{16}O+^{16}O$ are typical of an entire class of scattering systems, and are remarkable for three characteristics.

(1) *Internal transparency.* For small r values, W is typically 20 MeV deep, which is only 1/10–1/5 of V over the same r range. This implies deep, elastic interpenetration of the target and projectile, and is a feature unambiguously required by the appearance of nuclear rainbows in the angular distributions.

(2) *Far-surface transparency.* Both $V(r)$ and $W(r)$ have exponential tails, with the quite different decay lengths $a_V \sim 0.9$ fm and $a_W \sim 0.6$ fm, implying lower reaction rates in the far tail than the matter distribution might suggest: As a function of r, reactions fall off much more sharply than does the matter distribution for these systems.

(3) $W \approx V$ *in the near surface.* The pronounced maximum in $w(r)$, with a peak value in the range 0.5–1.3, occurs without exception for this class of scattering systems, over the wide energy per nucleon range 6 MeV$\lesssim E_L/A \lesssim$100 MeV. As the logarithmic plots of Fig. 1 make clear, the maximum is in part a consequence of the condition $a_W < a_V$.

This maximum in the $w(r)$ ratio is an intriguing feature of the potential systematics; as we indicate below, when it occurs, its location always seems to be very close to the ''strong absorption radius'' of the corresponding scattering system. The few data available at higher energy suggest that the far-surface transparency and, hence, also the $w(r)$ maximum disappear above approximately 100 MeV/nucleon. Furthermore, it is not universal even within this range: Counterexamples for which reliable potentials are available include the scattering of ^{20}Ne, ^{14}N, and ^{9}Be, all by a ^{12}C target.

III. UNIQUENESS OF THE POTENTIALS: *A* AND *E* RANGES COVERED

The potential systematics illustrated by Fig. 1 persist over the cited energy range 6 MeV$\lesssim E_L/A \lesssim$100 MeV, but have so far been found only for a rather narrow range of (target +projectile) combinations: $^{12,13}C+^{12}C$, $^{16}O+^{16}O$, $^{16}O+^{12}C$, $\alpha+X$ and $^{6}Li+X$ (where X ranges from ^{12}C to ^{208}Pb). This narrow range may be due in part to the fact that data at sufficiently large angles are not available for many more systems, but those for which reliable potentials are available, and are known to lie outside the $w(r)$ systematics, are $\alpha+^{116}$Sn, $^{20}Ne+^{12}C$, $^{14}N+^{12}C$, $^{9}Be+^{12}C$, and $^{9}Be+^{16}O$.

Because these systematics are seen much more clearly in the optical potentials than in the angular distributions themselves, the reliability and degree of uniqueness of these potentials are crucial and require some discussion. It is not claimed that the potentials included in this analysis are unique, energy by energy, for they are not. As recent analyses have made clear [9–12], a given set of elastic data will probably never determine an optical potential uniquely, in

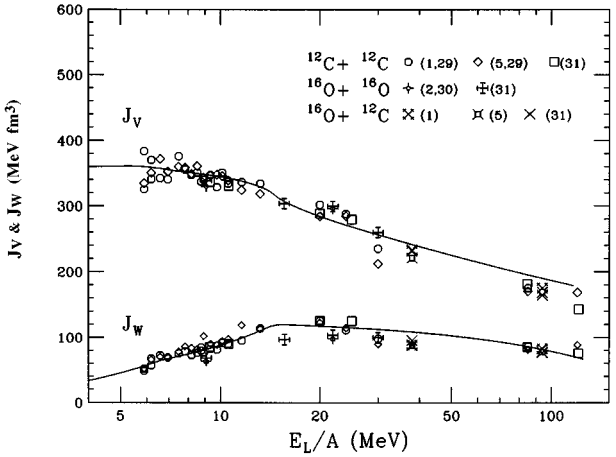

FIG. 2. Volume integrals per nucleon pair J_V and J_W as a function of laboratory energy per nucleon. The values are the result of phenomenological [1,29] and folding model [5,29,31] analyses of $^{12}C+^{12}C$, phenomenological [2,30] and folding model [31] analyses of $^{16}O+^{16}O$, and phenomenological [1] and folding model [5,31] analyses of $^{16}O+^{12}C$. Numbers in parentheses correlate symbols to references.

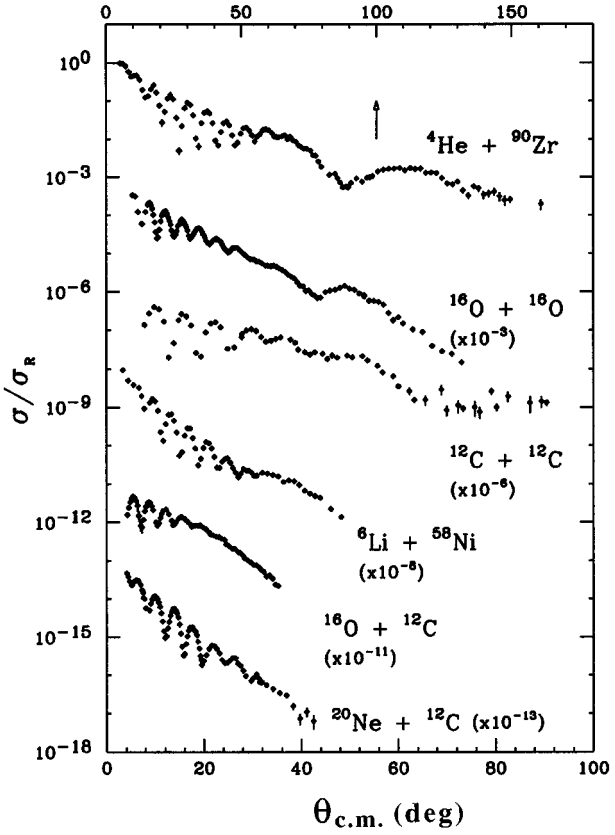

FIG. 3. Elastic scattering data of α scattering off ^{90}Zr at 20 MeV/nucleon [16], $^{16}O+^{16}O$ at 22 MeV/nucleon [15], $^{12}C+^{12}C$ at 13 MeV/nucleon [17], $^{6}Li+^{58}Ni$ at 35 MeV/nucleon [3], $^{16}O+^{12}C$ at 38 MeV/nucleon [18], and $^{20}Ne+^{12}C$ at 20 MeV/nucleon [19].

the sense that the fit to one set of data points can always be improved by adding more potential parameters, permitting ever more exotic shapes to the potential. What we do claim as unique for the potentials considered in this work is their smoothness and systematics as a function of energy. Guided in part by this criterion, we have restricted our considerations to a very specific class of potentials: the customary six-parameter Woods-Saxon (WS) potentials, extended in a few cases to include $(WS)^n$ and surface absorption, as well as a few ''microscopic'' or double-folding potentials. We have done so for two reasons: first, because these are the potentials which were originally found to provide impressive and physically significant fits to the data, and second because these ''simplest'' potentials fall into clear families, only one of which has parameters (and real and imaginary volume integrals) which vary smoothly and systematically with bombarding energy. Figure 2 shows, as an example of the systematics displayed by the real and imaginary volume integrals per interacting nucleon pair, the values of these quantities for three heavy-ion systems over a wide range of energies analyzed with a variety of phenomenological and microscopic potentials of the type considered in this analysis. At many individual energies these potentials may not be distinctly unique, but to the best of our knowledge they are the only ones which have a consistent dependence on the energy—a point to which we return at the end of this section.

As a reminder of the general features of the angular distributions which determine these potentials, Fig. 3 shows six typical examples, the first five of which produce potentials exhibiting the $w(r)$ systematics, while the last does not. All of them show near-side [13,14] dominance (from the long-range repulsive Coulomb interaction) at forward angles and far-side dominance (from the short-ranged attractive nuclear interaction) at larger angles. The near-far interference at intermediate angles produces the high-frequency Fraunhofer oscillations ($\Delta\theta \approx 1/kR$) that determine the radius of the absorptive part of the potential. Other essential features of these complex angular distributions are the angular position and width of this Fraunhofer diffraction region (determined by the relative sizes and slopes of the near-side and far-side amplitudes) and the position and depth of the broad far-side minimum (especially pronounced for $\alpha+^{90}Zr$ and $^{16}O+^{16}O$), if present at all. It is this combination of distinct features which suffices to fix uniquely the parameters of our standard Woods-Saxon potential,

$$V(r)=\frac{-V_0}{1+e^{(r-R)/a}}, \quad W(r)=\frac{-W_0}{1+e^{(r-R_i)/a_i}}. \tag{2}$$

The most important of these features, and certainly the one most clearly responsible for reliably determining the potential parameters, is the above-mentioned broad far-side dip seen most clearly in $^{16}O+^{16}O$ [15] and $\alpha+^{90}Zr$ [16], less clearly in $^{6}Li+^{58}Ni$ [3] (at about 30°) and $^{12}C+^{12}C$ [17], and not at all in either $^{16}O+^{12}C$ [18] or $^{20}Ne+^{12}C$ [19]. When present, this dip has been unambiguously identified as the Airy minimum of a nuclear rainbow, i.e., a destructive interference between two far-side trajectories which thoroughly sample the interior of the potential. It is these trajectories which unambiguously require the internal region of the potential for these systems to be ''transparent,'' i.e., $W_0/V_0 \lesssim 0.1$–0.2.

If this Airy minimum fails to appear, as in the $^{16}O+^{12}C$ angular distribution shown, the optical potential is not uniquely determined. In this case, as in several others [1,5], a χ^2 search does produce a distinctive local minimum with $W_0/V_0 \lesssim 0.2$, i.e., internal transparency, but in addition finds a wide range of equivalent fits to the data in which the potential interior is strongly absorbing, $W_0/V_0 \sim 0.5-1$ (''black interior'') [5]. Curiously, both $^{16}O+^{16}O$ and $^{12}C+^{12}C$ exhibit angular distributions which at some energies in the $E_L/A<100$ MeV range show unambiguous Airy dips, but at other, interleaved, energies show none [20]. At these latter energies the potential becomes ambiguous, but we have included these energies in our catalog of potential cases because it seems highly unlikely that $W_0(E)$ would jump from, say, 25 to 100 MeV as the bombarding energy went from 200 to 300 MeV, and then back again at 400 MeV. Consequently we have used the unambiguous shallow-W potentials at the energies where they are well determined, to argue that shallow-W potentials should also be chosen at those energies where the Airy minimum is ''missing''; the remarkable feature is not that these shallow-W potentials are unique, but that they exist at all, at every energy measured for these systems. This is the ''consistency criterion'' mentioned earlier in this section. In similar fashion, since both $^{16}O+^{16}O$ and $^{12}C+^{12}C$ so frequently exhibit shallow-W behavior, we have also chosen shallow-W solutions for the $^{16}O+^{12}C$ system, even though Airy minima are not apparent in either of the angular distributions which have been measured so far [21,18,22].

In this context of uniqueness, we note the extensive (and contrasting) work of Cooper and Mackintosh [10]. This work has produced multiparameter potentials, identified by the acronym PIPS, that provide significantly better fits to several of these same angular distributions, but which are entirely different, in many cases, from the potentials we include. In particular, in those distributions which do not exhibit a clear far-side Airy minimum, the PIPS $V(r=0)$ is often as much as a factor of 10 shallower than those of the WS potentials—yet when an Airy minimum does occur, it demands the deeper $V(r)$ for both the PIPS and WS potentials. In the most striking example, the excellent 350 MeV data for $^{16}O+^{16}O$ [15] forces the PIPS potential into exactly the deep-V WS class we have chosen, with a $w(r)$, shown in Fig. 6 below, nearly identical to those of the WS class. Thus the PIPS potentials exhibit an erratic energy dependence and no W/V systematics at all. This does not necessarily suggest that they are unphysical, but our purpose here is to analyze energy systematics, and for this reason we are driven to the Woods-Saxon-type potentials, which are smoother both in r and in energy.

The $^{20}Ne+^{12}C$ case shown, on the other hand, appears to define a limit to the $w(r)$ systematics. Although this angular distribution seems to be qualitatively similar to that for $^{16}O+^{12}C$, it is evidently different, for all attempts to fit the data have failed to turn up a potential of the type displayed in Fig. 1. The closest potential available [23], though of moderately shallow W ($W_0 = 35$ MeV), is not at all surface transparent and in fact has $|W(r)|>|V(r)|$ for $r>6$ fm. Similar results are found for $^{14}N+^{12}C$ [24], $^{9}Be+^{12}C$, and $^{9}Be+^{16}O$ [25]. Thus the W/V systematics, though persistent over a wide energy range for several light systems, are not universal.

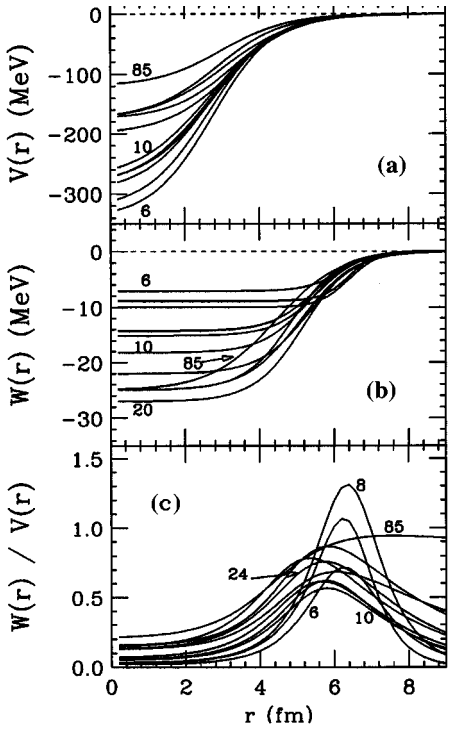

FIG. 4. Phenomenological (Woods-Saxon) potentials for $^{12}C+^{12}C$ [29]. (a) Real parts, (b) imaginary parts, and (c) ratios. Numbers indicate laboratory energy per nucleon, in MeV.

IV. $w(r)$ SYSTEMATICS

The above examples make it clear that the $w(r)$ systematics, though immediately obvious as a property of the optical potentials, are well camouflaged in the angular distributions, unless they exhibit clear nuclear rainbows. The systematics are *potential* systematics, which we explore in some detail in this section.

A. Preliminaries

$^{12}C+^{12}C$ is a typical example. Figures 4(a) and 4(b) show $V(r)$ and $W(r)$ over a wide enough energy range that the potential for the highest-energy case ($E_L=1016$ MeV, $E_L/A=85$ MeV) violates the systematics by having $W(r)\approx V(r)$ in its tail. This is clearer from Fig. 4(c), which shows the corresponding $w(r)$ curves. The optical potential for $^{12}C+^{12}C$ is clearly not static: V_0, e.g., decreases from 330 to 115 MeV over the bombarding energy range 6 MeV $<E_L/A<85$ MeV, while W_0 increases from 7 to 27 MeV. In spite of these large changes in the potential parameters, Fig. 4(c) shows the shape of $w(r)$ to remain remarkably stable, via appropriately correlated variations in the geometrical parameters. In fact, the maximum in $w(r)$ actually reaches its largest value of about 1.3 for one of the lowest bombarding energies, where W_0 is small and V_0 large. As can be observed in the figure, at energies where a maximum exists, its location moves to smaller radii as the energy increases.

Although it is this maximum in $w(r)$ which first strikes the eye, the maximum appears to us to be less significant than the *small* values of $w(r)$ at large and small r, which physically describe unusual transparency. In this context, it is perhaps worthwhile inquiring under what conditions $w(r)$ has a maximum at all, since there are certainly potentials for which it is monotonically increasing, with no maximum. Taking the WS shapes of Eq. (2) as a representative example, $w'(r)=0$ yields the condition

$$\frac{a}{a_i}=\frac{1+e^{-(r-R_i)/a_i}}{1+e^{-(r-R)/a}}\equiv\mathcal{R}(r), \tag{3}$$

which will have a solution for $r>0$ if the maximum is present. Although there are several ways in which this equation can be satisfied at a maximum, it is intuitively obvious from Fig. 1 that $a_i<a$ is a necessary condition, and indeed the potentials satisfying the $w(r)$ systematics all have

$$R_i>R, \quad a_i<a, \tag{4}$$

which make the left-hand side of Eq. (3) greater than 1. The right-hand side $\mathcal{R}(r)$ then has the value

$$\mathcal{R}(0)=\frac{1+e^{R_i/a_i}}{1+e^{R/a}}>1 \tag{5}$$

at $r=0$ and descends through 1 at

$$r_1=\frac{aR_i-a_iR}{a-a_i}. \tag{6}$$

Hence the two sides can be equal for some r between 0 and r_1. This is exactly what happens for potentials of the systematics type, whose parameters typically satisfy $a/a_i \sim 1.6$, $R_i/a_i \sim 7$, and $R/a \sim 3$.

Thus the essential conditions which produce the $w(r)$ maximum for these potentials are those of Eq. (4), $R_i>R$ and $a_i<a$; the appearance of a maximum is not affected by the value of W_0/V_0, though the height of the maximum is, of course, proportional to it. Under these conditions, the maximum occurs at an r value slightly larger than R_i. This is illustrated in Fig. 5, which compares $w(r)$ with dW/dr (which peaks at $r=R_i$) for potentials that describe three different systems. We extend the comparison by displaying in addition $d|S|/d\ell$, where $S(\ell)=e^{2i\delta(\ell)}$ is the S-matrix element for a given potential, and we plot it as a function of $r(\ell)$ by taking r as the distance of closest approach for a given trajectory, found numerically from

$$\ell=rk(r)=rk_\infty\left[1-\frac{V(r)+V_{\rm Coul}}{E_{\rm c.m.}}\right]^{1/2}. \tag{7}$$

$d|S|/d\ell$ also peaks slightly outside of dW/dr, because of the longer-ranged attraction $V(r)$, which pulls flux into the $W(r)$ absorption from large r values that would otherwise have missed it altogether. In accordance with the Austern-Blair [26] approximation, $d|S|/d\ell$ provides an indication of the peripheral radial region in which collective direct reactions originate, and its peak marks the so-called ''strong absorption radius'' for the system. It is curious, and perhaps significant, that whenever $w(r)$ has a maximum, it occurs very close to this strong absorption radius, slightly outside $r=R_i$. This is true both for different systems and for different energies.

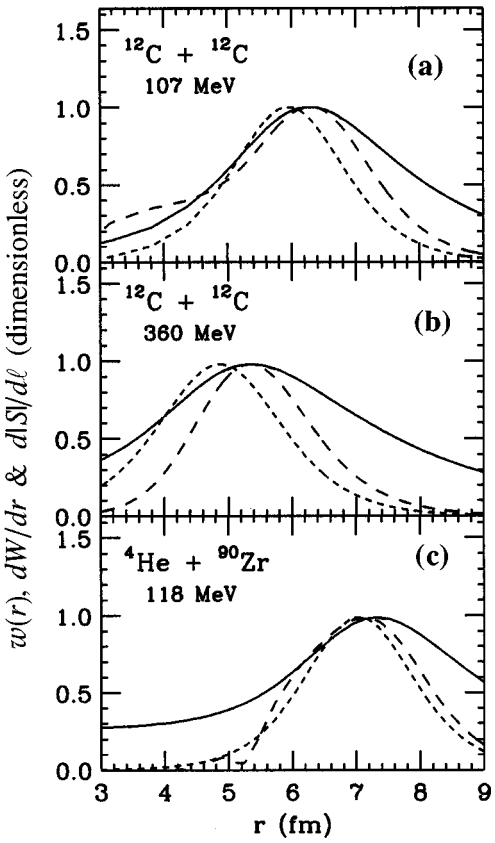

FIG. 5. $w(r)$ (solid line), dW/dr (short dashed line), and $d|S|/d\ell$ (long dashed line) for three different systems. All curves have been normalized to 1.0 at their peaks.

Since the transparency of the far-tail region plays such an important role in defining the W/V systematics, it is worth emphasizing that this transparency is unambiguously demanded by these experimental angular distributions, as we have verified by a variety of notchlike tests. In fact, the far-tail transparency is even found to be a feature of the deep-W potentials [5] for ^{16}O+^{12}C at 608 MeV (the ones we have not included here), whose $w(r)$ decreases monotonically, without a maximum.

B. Main body of the $w(r)$ systematics

In order to conveniently compare $w(r)$ curves for scattering systems of differing sizes, we plot them versus the scaled radius

$$r_0\equiv\frac{r}{A_1^{1/3}+A_2^{1/3}}, \tag{8}$$

rather than versus r, recalling that for the real and imaginary parts of the potentials, typical empirical r_0 radial parameters are

$$r_0(V)\approx 0.7 \text{ fm}, \quad r_0(W)\approx 1.1 \text{ fm}. \tag{9}$$

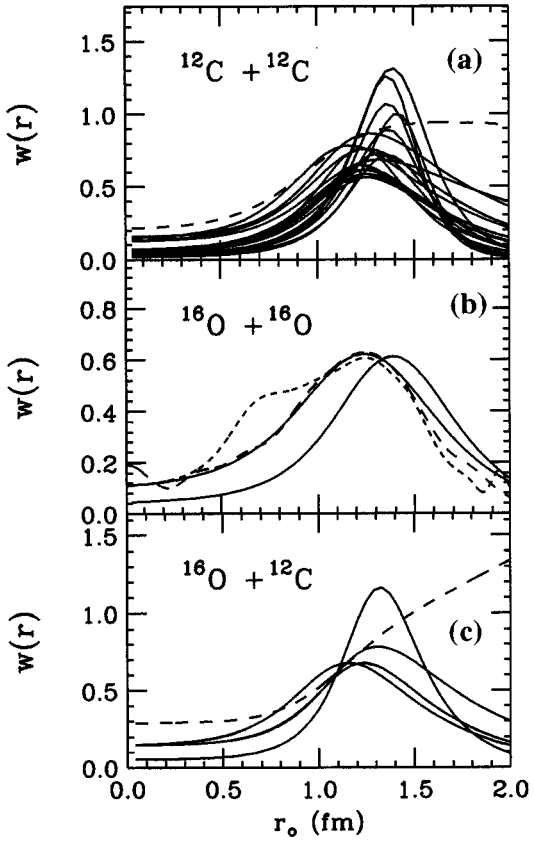

FIG. 6. Ratios $w(r)$ versus the reduced radius for systems that follow the systematics. In (a), different curves correspond to phenomenological potentials (Woods-Saxon) at different energies [1,29]; the dashed line is for 85 MeV/nucleon. In (b), $w(r)$ for potentials at 145 and 350 MeV. Solid curves are ratios for phenomenological potentials (Woods-Saxon squared) at each energy [30,2]; dashed curves are ratios for two PIPS potentials obtained at 350 MeV by inversion [10]. In (c), phenomenological potentials (Woods-Saxon) at different energies [1]; the dashed curve corresponds to 94 MeV/nucleon.

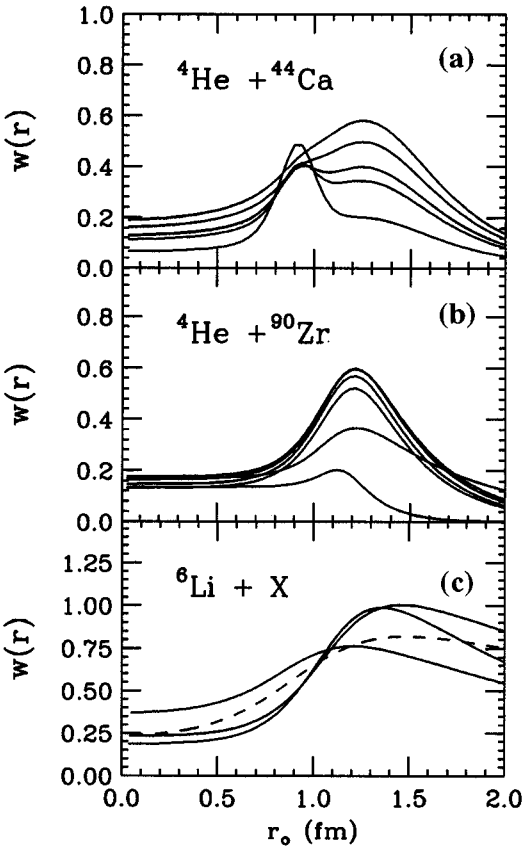

FIG. 7. Ratios $w(r)$ for other systems that follow the systematics, at different energies. In (a), phenomenological potentials (Woods-Saxon squared plus Woods-Saxon squared derivative) at α energies between 24 and 100 MeV [32]. In (b), Woods-Saxon potentials between 40 and 142 MeV [16]. In (c), solid curves correspond to Woods-Saxon potentials at 35 MeV/nucleon for ^{6}Li on ^{12}C, ^{40}Ca, and ^{58}Ni targets [3,4]; dashed curve is for ^{6}Li+^{12}C at 53 MeV/nucleon [36].

By far the most extensively studied system is ^{12}C+^{12}C. Reliable potentials for it are available [27,28,1,29] at a large number of energies, 20 of which are represented in the $w(r)$ curves of Fig. 6(a). With the single exception of the highest-energy ($E_L/A=85$ MeV) data, all show distinct peaks centered in the $r_0=1.2-1.4$ fm range. The ^{16}O + ^{16}O [2,30,31] potentials are similarly very reliable because of the prominent rainbows in the data. Only two sets of measurements have so far been published (those at 250 and 350 MeV; at 124, 480, and 704 MeV they have been preliminarily reported), and their $w(r)$ curves, shown in Fig. 6(b), are very similar to the ^{12}C+^{12}C results, as are the shallow-W curves for ^{16}O+^{12}C [1] shown in Fig. 6(c), with the exception of their highest-energy case. The lowest-energy ^{4}He + ^{44}Ca curves [32], Fig. 7(a), are somewhat unusual in having an ''extra'' maximum [from a corresponding sharp maximum in $W(r)$ itself] at $r_0\approx0.9$ fm, which may arise from excitation of the four valence nucleons of ^{44}Ca; it is not present in ^{4}He+^{40}Ca. The ^{4}He+^{90}Zr curves [16] of Fig. 7(b) and those for ^{6}Li+X [3,4] in Fig. 7(c) all follow the $w(r)$systematics, over the energy range available, the highest energy showing the previously observed tendency for the $w(r)$ peak to become extremely wide.

By way of contrast, Fig. 8(a) shows a few intermediate-energy examples for ^{20}Ne+^{12}C, ^{14}N+^{12}C, ^{9}Be+^{12}C, and ^{9}Be+^{16}O, all of which have $a_i>a$ and so are far-surface absorptive, with a $w(r)$ curve which is monotonic increasing, with no maximum. In particular, the optical model analysis of ^{14}N+^{12}C at 20 MeV/nucleon [24] offered two possible descriptions of the data, one in terms of a ''shallow'' imaginary potential [$W(0)=26.9$ MeV] and another with a ''deep'' imaginary part [$W(0)=67.9$ MeV]. Both types of potentials have a relatively large imaginary diffuseness ($a_i\approx0.9$ fm) and do not follow the systematics; apparently, this feature is required by the measurements. Another situation is found in α+^{116}Sn shown in Fig. 8(b). Exactly what it is about the structure of these nuclei that sets them apart from the previous ''α-particle nuclei'' is not yet clear, but the mere fact that they deviate so strongly from the $w(r)$ systematics indicates that the detailed structure of target and projectile influences the absorptive part of their optical potential. Although the simple folding procedure is adequate for $V(r)$, it is entirely incorrect for $W(r)$ [8]. Data for the systems in Fig. 8(a) exist only at single energies; conse-

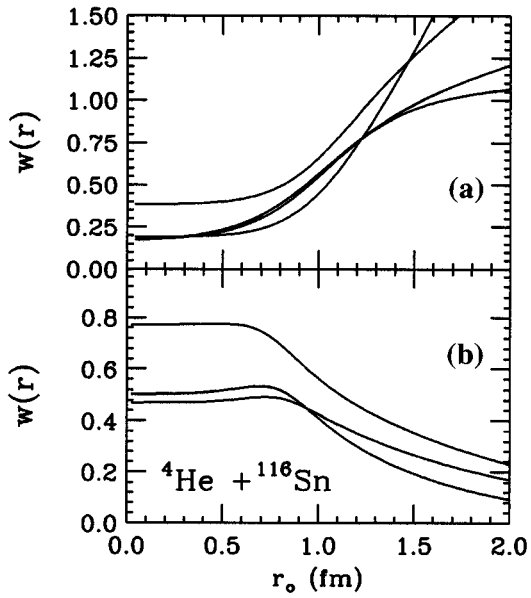

FIG. 8. Ratios $w(r)$ for systems that do not follow the systematics. In (a), ^{20}Ne+^{12}C at 20 MeV/nucleon [23], ^{9}Be+^{12}C and ^{9}Be+^{16}O at 18 MeV/nucleon [25], and ^{14}N+^{12}C at 20 MeV/nucleon [24]. In (b), alpha particles off ^{116}Sn between 72 and 120 MeV/nucleon [37].

quently, no information is available on the energy dependence of their potentials.

We point out that the microscopic potentials [folding model $V(r)$, phenomenological WS $W(r)$] for ^{12}C+^{12}C between 6 and 85 MeV/nucleon frequently violate the W/V systematics. The example included in Fig. 1(b) happens to be a case in which w does present a well-defined peak, but this peak tends to disappear, for these potentials, above 10 MeV/nucleon. In terms of potential parameters, this is explained by the fact that the real ''diffuseness,'' determined in this case by the ingredients entering the double-folding procedure (choice of the DDM3Y effective interaction [33] and parametrization of the ^{12}C density distribution), is comparable to or smaller than the phenomenological imaginary diffuseness required by the fit. A recent study by Satchler [9] has addressed in detail the issue of the optimum shape for the real part of the potential, in particular for the ^{16}O+^{12}C data at 608 MeV. The use of splines in addition to the DDM3Y potential led to the conclusion [9] that the tail of the folding model real part is too steep, possibly due to the simplified treatment of the nucleon exchange term; a potential tail extending further out improves the description of these data. The comparison between the microscopic and phenomenological ^{12}C+^{12}C real potentials depicted in Figs. 1(a) and 1(b) shows good agreement in the interior and differences beyond $\approx$5 fm; in this case, too, the folding real part is steeper than the phenomenological result, differing by about 40% at 6 fm. A qualitatively similar result is observed at other energies. This suggests that the conclusions [9] for ^{16}O+^{12}C at 608 MeV might be generalized to similar systems and, therefore, could explain this exception to the w systematics as due to a limitation of the form of the DDM3Y interaction.

V. IMPLICATIONS FOR THE GLAUBER APPROXIMATION

The preceding article [34] demonstrated that in the energy range $E_L/A < 100$ MeV, the ''optical limit'' of the double-Glauber approximation fails completely to describe nucleus-nucleus scattering in terms of nucleon-nucleon scattering amplitudes. The problem is not in the use of the eikonal approximation, but rather in the ''Glauber potential'' employed for the optical phase shifts, which is nothing more than the above-mentioned double-folding potential, employed for $W(r)$ as well as for $V(r)$, with complete neglect of Pauli blocking. This potential not only gives $V(r)$ and $W(r)$ the same radial shape, but even makes them approximately equal [i.e., $w(r)\approx 1$] in the energy range below 100 MeV/nucleon.

As the above examples of $w(r)$ make clear, this grossly overestimates the absorption in this energy range, but the few angular distributions available at somewhat higher energies do suggest that $w(r)\approx 1$ in the far-surface region, even for ^{12}C and ^{16}O nuclei, at these energies. Since the density is the lowest in the surface, where the nucleons are closest to being free and the local Fermi energy is low, Pauli blocking should be minimal, and it is plausible that the double-folding procedure should be most reliable there for $W(r)$. If so, this suggests that the increased absorption implied by $w(r)\approx 1$ in the far surface may be due to an increased probability there of nucleon knockout, which is the only form of absorption included in the Glauber description.

At sufficiently high energy, where the bombarding energy is much larger than the total (target+projectile) binding energy, one expects that all nuclear binding effects should become negligible and that the double-Glauber approximation should become accurate for all phase shifts, even the low-ℓ ones. Consequently we conjecture that $E_L/A \sim 100$ MeV may be the transition energy range, where this approximation begins to be accurate at large ℓ (large r) and that the appearance of optical potentials with $w(r)\approx 1$ in the far surface may be an indication of this. If so, this would make heavy-ion optical potentials at these 100 MeV/nucleon energies exceptionally interesting, since their $w(r)$ curves could provide direct evidence of the density dependence of Pauli blocking. This would imply, in particular, that

$$w(r)\approx \alpha^{-1}\equiv \mathrm{Im}[f_{NN}(0^\circ)]/\mathrm{Re}[f_{NN}(0^\circ)] \qquad (10)$$

at large r values, where Pauli blocking is weak. Further,

$$\Delta(r)\equiv \alpha^{-1} - w(r) \qquad (11)$$

could then serve as a measure of the Pauli blocking at smaller r values, where the higher nucleon density implies higher local Fermi momenta. However, accurate $\Delta(r)$'s require accurate potentials, and all past experience suggests that reliable optical potentials can only be determined by accurate large-angle data, extending in angle well beyond the near-far crossover region of Fraunhofer oscillations.

VI. SUMMARY AND DISCUSSION

The body of data summarized by the $w(r)$ curves of Sec. IV is very large, and the stability of these curves over such a

range of energies and of heavy-ion systems suggests that it may carry an important message. We conjecture that the essence of this message lies in the small values of $w(r)$ at both large and small r values, for systems like $^{12}C+^{12}C$ and $^{16}O+^{16}O$, at energies below 100 MeV/nucleon. These small w's imply a substantial suppression of reactions in these regions, relative to systems like $^{20}Ne+^{12}C$ as well as to the $w(r)=\alpha^{-1}\approx 1$ predicted by free nucleon-nucleon scattering in the optical limit of the double-Glauber approximation. In particular, the far-surface reactions which do take place in systems like $^{20}Ne+^{12}C$ below 100 MeV/nucleon, and possibly in all heavy-ion systems at higher energies, occur outside the r range in which peripheral transfer and collective-inelastic reactions originate, and so must represent other forms of absorption.

In this connection we recall an early work on low-energy $^{20}Ne+^{12}C$ and $^{16}O+^{16}O$ elastic scattering [35] which found a much larger absorption in the first of these systems. The authors suggested that angular momentum matching conditions might explain the difference, by favoring the $^{20}Ne+^{12}C$ direct reaction channels over those for $^{16}O+^{16}O$. Even if the explanation is only valid at the energy it was applied to, it indicates important differences in the absorption properties of these two systems arising from details of their nuclear structure.

In an attempt to understand the $w(r)$ systematics, we offer two conjectures, both subject to experimental test. The first is that the far-surface reactions which appear above 100 MeV/nucleon are largely nucleon knockout, the only reaction mode included in the Glauber NN-scattering model. Glauber predicts $w(r)=\alpha^{-1}\approx 1$ for this mode, with α given by Eq. (10). Values of $w(r)$ larger than 1, which sometimes occur, would then imply the presence of other reaction modes as well.

The second conjecture is that the small values of $w(r)$ $[w(r)\ll\alpha^{-1}]$ seen at interior r values for ''α-particle nuclei'' may be due to Pauli blocking, in which case

$$\Delta(r)\equiv\alpha^{-1}-w(r) \tag{12}$$

could serve as a measure of this effect, as a function of r, i.e., of local density. If this is indeed the cause of the small internal values of $w(r)$, their suppression should diminish with increasing bombarding energy above 100 MeV/nucleon.

Independently of their interpretation, the existence of the $w(r)$ systematics carries substantial implications for the many radioactive beam experiments currently being planned. The interesting question is the degree of transparency that can be expected in systems formed by an exotic projectile, and the influence of this transparency on the corresponding optical potential. The systematics presented here should serve as a reminder that the potentials on which they are based were obtained only by measuring small cross sections at large angles, well beyond the Fraunhofer crossover region. Since it is unlikely that radioactive beams of a quality adequate for such measurements will ever be available, it is equally unlikely that unambiguous optical potentials for radioactive nuclei will be determined. One plausible means of reducing these potential ambiguities would be to extrapolate (most reliably the real part) from well-known potentials for stable nuclei. For such a purpose, systematics of the type described here would be extremely helpful. Consequently we suggest that programs of radioactive beam studies would be well advised to include a parallel program of elastic scattering of nearby stable nuclei on the same targets.

Preliminary reports of these results have been presented elsewhere [38–40].

ACKNOWLEDGMENTS

This project was partially funded by CONACYT-Mexico, Grant No. 3173E. K.W.M. gratefully acknowledges the gracious hospitality extended to him, during an essential part of this work, by the Instituto de Física of the UNAM.

[1] M. E. Brandan, Phys. Rev. Lett. **60**, 784 (1988).
[2] Y. Kondo *et al.*, Phys. Lett. B **242**, 340 (1990).
[3] A. Nadasen *et al.*, Phys. Rev. C **37**, 132 (1988).
[4] A. Nadasen *et al.*, Phys. Rev. C **39**, 546 (1989).
[5] M. E. Brandan and G. R. Satchler, Nucl. Phys. **A487**, 477 (1988).
[6] M. E. Brandan, S. H. Fricke, and K. W. McVoy, Phys. Rev. C **38**, 673 (1988).
[7] G. R. Satchler, *Direct Nuclear Reactions* (Oxford Universty Press, New York, 1983).
[8] G. R. Satchler and W. G. Love, Phys. Rep. **55**, 183 (1979).
[9] G. R. Satchler, Nucl. Phys. **A574**, 575 (1994).
[10] S. G. Cooper and R. S. Mackintosh, Nucl. Phys. **A576**, 308 (1994).
[11] M. E. Brandan and G. R. Satchler, Phys. Lett. B **256**, 311 (1991).
[12] M. E. Brandan, K. W. McVoy, G. R. Satchler, Phys. Lett. B **281**, 185 (1992).
[13] R. C. Fuller, Phys. Rev. C **12**, 1561 (1975).
[14] M. S. Hussein and K. W. McVoy, Prog. Part. Nucl. Phys. **12**, 103 (1984).
[15] E. Stiliaris *et al.*, Phys. Lett. B **223**, 291 (1989); HMI Annual Report 1989, HMI-B-482, p. 50.
[16] L. W. Put and A. M. J. Paans, Nucl. Phys. **A291**, 93 (1977).
[17] S. Kubono *et al.*, Phys. Rev. C **31**, 2082 (1985).
[18] M. E. Brandan *et al.*, Phys. Rev. C **34**, 1484 (1986).
[19] H. G. Bohlen *et al.*, Z. Phys. A **346**, 189 (1993).
[20] K. W. McVoy and M. E. Brandan, Nucl. Phys. **A542**, 295 (1992).
[21] M. E. Brandan and A. Menchaca-Rocha, Phys. Rev. C **23**, 1272 (1981).
[22] P. Roussel *et al.*, Phys. Rev. Lett. **54**, 1779 (1985).
[23] M. E. Brandan (unpublished). The parameters for this standard Woods-Saxon potential are 91.7 MeV, 4.38 fm, 0.830 fm, 35.0 MeV, 5.20 fm, and 0.917 fm.
[24] M. E. Brandan *et al.*, Phys. Rev. C **42**, 2236 (1990).
[25] G. R. Satchler *et al.*, Phys. Lett. **128B**, 147 (1983).
[26] N. Austern and J. S. Blair, Ann. Phys. (N.Y.) **33**, 15 (1965).

[27] H. G. Bohlen *et al.*, Z. Phys. A **322**, 241 (1985).
[28] M. Buenerd *et al.*, Nucl. Phys. **A424**, 313 (1984).
[29] M. E. Brandan, M. Rodríguez-Villafuerte, and A. Ayala, Phys. Rev. C **41**, 1520 (1990).
[30] Y. Sugiyama *et al.*, Phys. Lett. B **312**, 35 (1993).
[31] D. T. Khoa *et al.*, Phys. Rev. C **49**, 1652 (1994).
[32] Th. Delbar *et al.*, Phys. Rev. C **18**, 1237 (1978).
[33] M. El-Azab Farid and G. R. Satchler, Nucl. Phys. **A438**, 525 (1985).
[34] M. E. Brandan, H. Chehime, and K. W. McVoy, Phys. Rev. C **55**, 1353 (1997), the previous paper.
[35] R. Vandenbosch, M. P. Webb, and M. S. Zisman, Phys. Rev. Lett. **33**, 842 (1974).
[36] A. Nadasen *et al.*, Phys. Rev. C **47**, 674 (1993).
[37] B. Bonin *et al.*, Nucl. Phys. **A445**, 381 (1985).
[38] K. W. McVoy and H. Chehime, Rev. Mex. Fis. **40**, Suppl. 1, 144 (1994).
[39] M. E. Brandan, in *Heavy-Ion Dynamics and Hot Nuclei*, 1995 ACS Nuclear Chemistry Award, Anaheim, California, edited by G. Nebbia and M. N. Namboodiri (World Scientific, Singapore, 1995), p. 193.
[40] M. E. Brandan, in *Low Energy Nuclear Dynamics*, XV Nuclear Physics Divisional Conference, St. Petersburg, Florida, 1995, edited by Yu. Onganessian, W. von Oertzen, and R. Kalpakchieva (World Scientific, Singapore, 1995), p. 399.